GSA DATA REPOSITORY 2015269

Supplemental Material for:

Late stage formation of martian chloride salts through ponding and evaporation

Brian M. Hynek, Mikki K. Osterloo, and Kathryn S. Kierein-Young

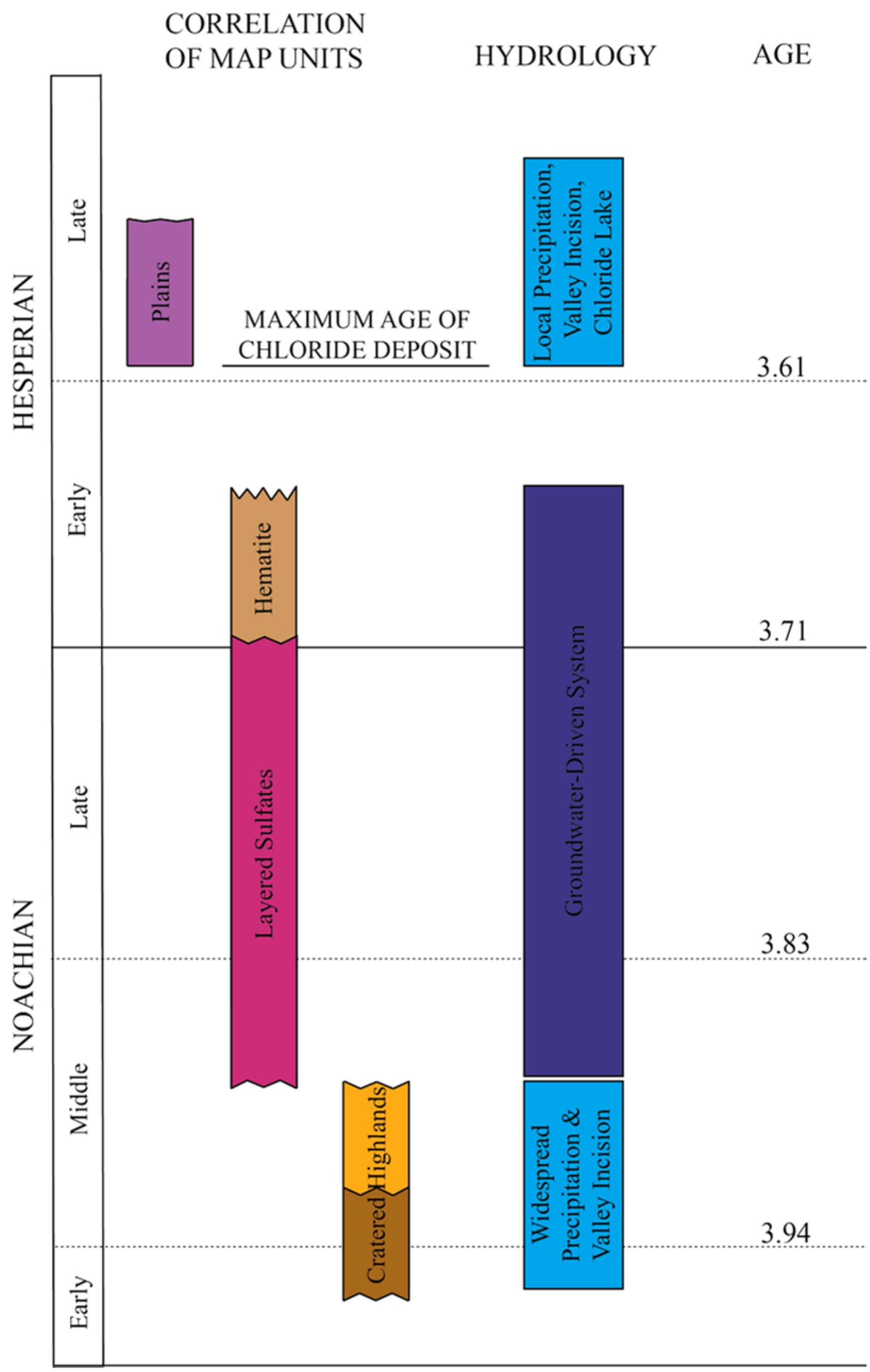

Figure DR1. Modified correlation of map units from geologic map of Hynek and di Achille (2015) in Figure 1. Also shown are the hydrologic history and maximum age of the chloride deposit. Martian epoch lower boundary ages are from Michael (2013).

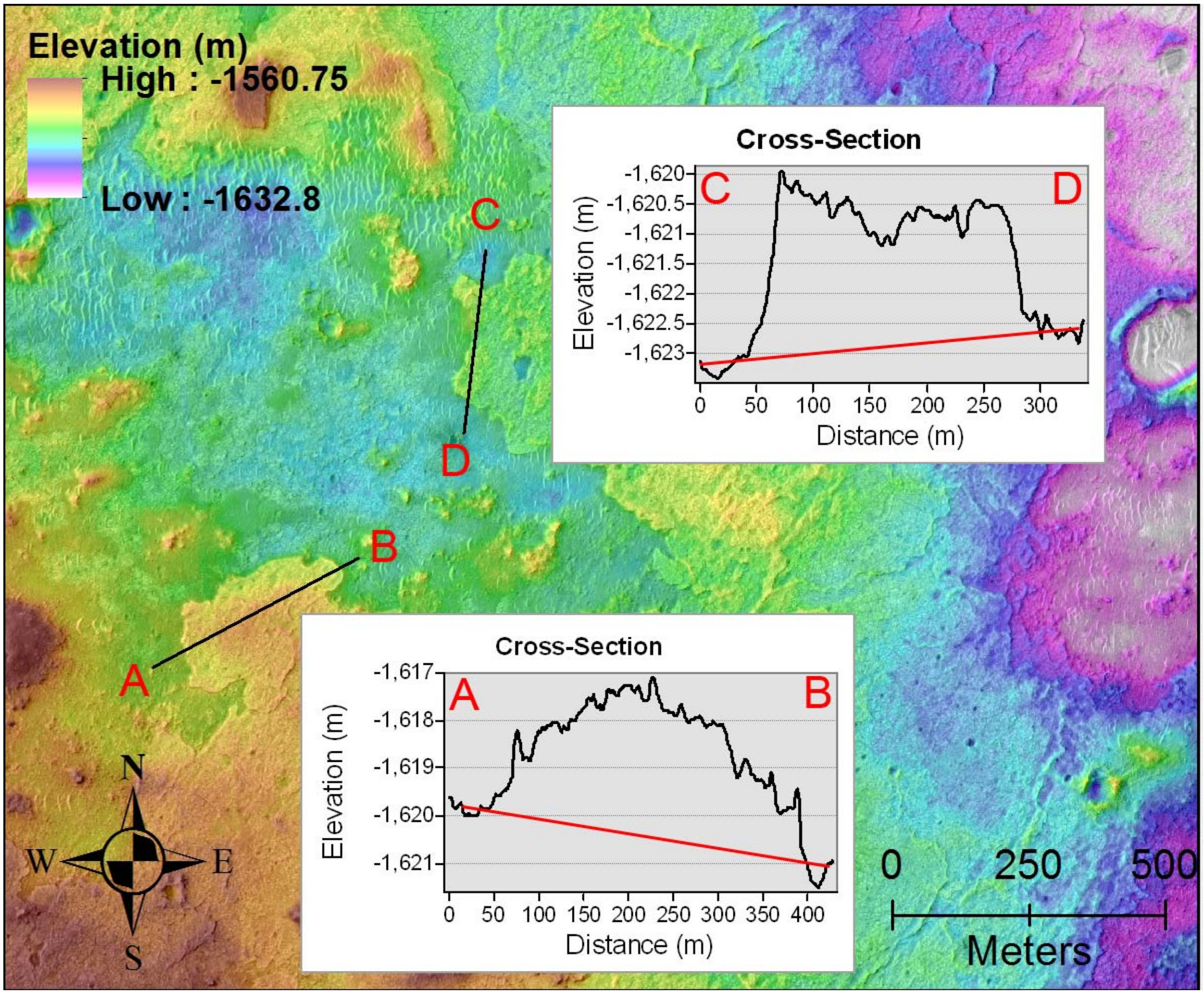

Figure DR2. Digital terrain model centered at 3.1°S, 8.5°W of erosional edges of light toned chloride deposits created from the HiRISE image cubes PSP_008917_1770_RED and PSP_007770_1770_RED. The cross-sectional profiles constrain the thickness of the chloride deposit in this region to less than 3 m. Red lines indicate the trend of the underlying surface.

Detailed Spectroscopic Methodology:

We used a full resolution (frt0000b2d0_07_if165l_trr3, 18 m/pix) image from the Compact Reconnaissance Imaging Spectrometer for Mars (CRISM) instrument for our spectroscopic characterization (Murchie et al, 2007). We applied the standard photometric and atmospheric corrections using the volcano scan method (McGuire et al, 2009). We then applied an adaptive spectral filter to remove single band spurious noise spikes. This filter uses a moving kernel of 5 bands in the spectral dimension. If the center value within the kernel was more than a single standard deviation away from the kernel's mean, then the center value is replaced with the mean. The kernel is then moved one spectral band and statistics are recalculated. The adaptive spectral filter was applied to each spectrum in the data set and smoothes the spectra by removing single band spikes. We examined the location of spectral absorption features before and after the adaptive filtering to ensure that no feature positions were affected. Figure S3A shows a CRISM spectrum for a single pixel before and after the adaptive spectral filter.

We examined filtered CRISM images and spectra to identify minerals within the scene. Spectra for the chloride deposit are featureless except for a positive slope, consistent with the results of Glotch et al. (2010). Other bright areas in the image contain spectra that best match library spectra of nontronite, a Mg/Fe phyllosilicate, with an absorption band at 2.29 and a shoulder at 2.24 μm. Figure S3B shows averaged spectra for the chloride (blue) and nontronite (red) seen in Figure 2 as well as a library spectrum of nontronite (green) from Clark et al. (2007). Both CRISM spectra were divided by an averaged neutral spectrum from the same column to reduce residual instrument artifacts.

In order to map the extent of the chloride and phyllosilicate deposits, we divided the scene by a single average spectrum of a spectrally neutral region instead of the typical column spectra. This step provides a single correction for the entire image to reduce residual atmospheric and instrument artifacts without introducing striping. Striping occurs due to column differences in gain when dividing by column spectra because it is difficult to find consistent neutral regions across the entire image. We mapped the chloride and nontronite deposits in the corrected CRISM scene using an orthogonal subspace projection (OSP) technique (Harsanyi and Chang, 1994). We input spectra into the OSP mapping technique that finds the ideal subspace projection, which maximizes the difference between the spectra. The data from the scene was transformed into this subspace, and a matched filter was used to map the areas containing spectra matching the regions of interest. The OSP technique outputs relative abundance image maps for each region of interest where an abundance of one perfectly matches the input spectrum. The output images are stretched such that only relative abundances above zero are shown as matches to the input spectra. For this study, we input average spectra for two regions of interest, the chloride deposit and nontronite, into the OSP using bands between 1.05 to 2.6 μm in order to produce the scene maps (Figure S3B). The results of the OSP indicate that the chloride deposit is a large contiguous deposit and the nontronite deposits outcrop as small eroded knobs (Figure 2).

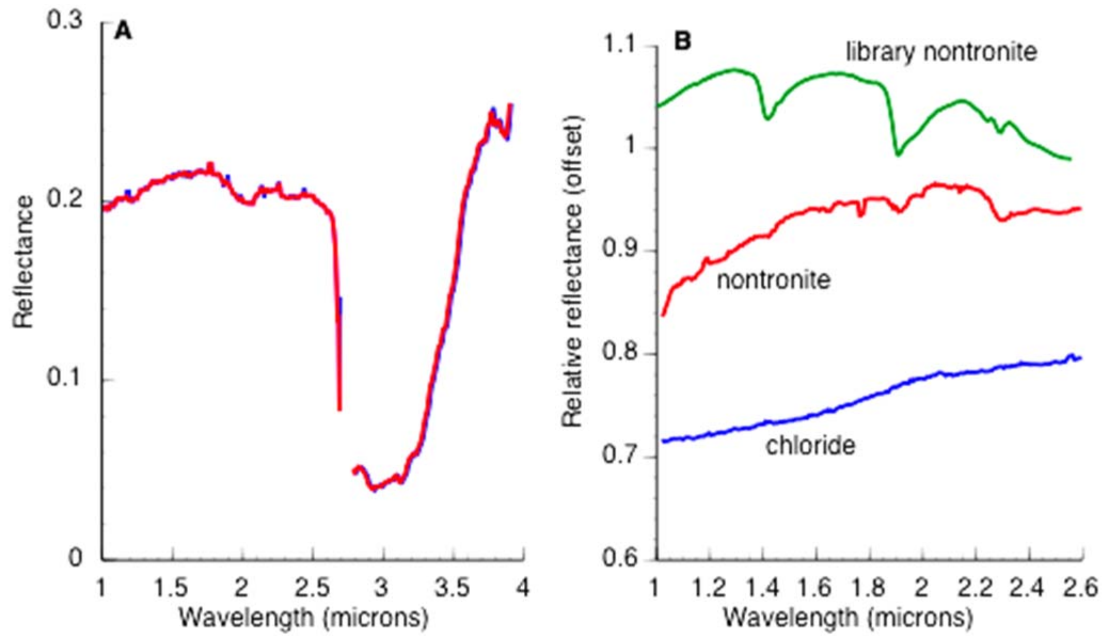

Figure DR3. (A) CRISM spectrum for a single pixel before and after the adaptive spectral filter (raw shown in blue, cleaned spectrum in red). (B) Average spectra for two regions of interest, the chloride deposit and nontronite library spectrum from Clark et al. (2007).

References

Clark, R.N., Swayze, G.A., Wise, R., Livo, E., Hoefen, T., Kokaly, R., and Sutley, S.J., 2007, USGS digital spectral library splib06a: U.S. Geological Survey, Digital Data Series 231.

Glotch, T.D., Bandfield, J.L., Tornabene, L.L., Jensen, H B., and Seelos, F.P., 2010, Distribution and formation of chlorides and phyllosilicates in Terra Sirenum, Mars: Geophysical Research Letters, v. 37, n. 16.

Harsanyi, J.C., and Chang, C.I., 1994, Hyperspectral image classification and dimensionality reduction: An orthogonal subspace projection approach: IEEE Transactions on Geoscience and Remote Sensing, v. 32, p. 779–785.

McGuire, P.C., et al., 2009, An improvement to the volcano-scan algorithm for atmospheric correction of CRISM and OMEGA spectral data, Planetary and Space Sciences, v. 57, 809–815, doi:10.1016/j.pss.2009.03.007.

Michael, G.G., 2013, Planetary surface dating from crater size–frequency distribution measurements: Multiple resurfacing episodes and differential isochron fitting: Icarus, v. 226(1), 885-890.

Murchie, S., Arvidson, R., Bedini, P., Beisser, K., Bibring, et al., 2007. Compact reconnaissance imaging spectrometer for Mars (CRISM) on Mars reconnaissance orbiter (MRO): Journal of Geophysical Research: Planets, v. 112, n. E5.